J Appl Electrochem (2011) 41:1261–1267
DOI 10.1007/s10800-011-0330-z

ORIGINAL PAPER

The compatibility of transition metal oxide/carbon composite anode and ionic liquid electrolyte for the lithium-ion battery

Shu-Lei Chou · Lin Lu · Jia-Zhao Wang · M. M. Rahman · Chao Zhong · Hua-Kun Liu

Received: 5 March 2011 / Accepted: 12 June 2011 / Published online: 12 July 2011

Abstract Three types of transition metal oxide/carbon composites including Fe_2O_3/C, NiO/C and CuO/Cu_2O/C synthesized via spray pyrolysis were used as anode for lithium ion battery application in conjunction with two types of ionic liquid: 1 M $LiN(SO_2CF_3)_2$ (LiTFSI) in 1-ethyl-3-methyl-imidazolium bis(fluorosulfonlyl)imide (EMI-FSI) or 1-methyl-1-propylpyrrolidinium bis(fluorosulfonyl)imide (Py13-FSI). From the electrochemical measurements, the composite electrodes using Py13-FSI as electrolyte show much better electrochemical performance than those using EMI-FSI as electrolyte in terms of reversibility. The Fe_2O_3/C composite shows the highest specific capacity and the best capacity retention (425 mAh g^{-1}) under a current density of 50 mA g^{-1} for up to 50 cycles, as compared with the NiO/C and CuO/Cu_2O/C composites. The present research demonstrates that Py13-FSI could be used as an electrolyte for transition metal oxides in lithium-ion batteries.

Keywords Ionic liquid · Anode · Transition metal oxide · Carbon composite · Lithium ion battery

S.-L. Chou · L. Lu · J.-Z. Wang · M. M. Rahman · C. Zhong · H.-K. Liu
Institute for Superconducting and Electronic Materials, University of Wollongong, Wollongong, NSW 2522, Australia

S.-L. Chou (✉) · J.-Z. Wang (✉) · M. M. Rahman · C. Zhong · H.-K. Liu
ARC Center of Excellence for Electromaterials Science, University of Wollongong, Wollongong, NSW 2522, Australia
e-mail: shulei@uow.edu.au

J.-Z. Wang
e-mail: jiazhao@uow.edu.au

1 Introduction

Rechargeable lithium-ion batteries currently dominate the power supply market for portable electronic devices [1]. The current lithium-ion batteries need to be further improved in both energy density and safety aspects to maintain their leading battery position [2]. Transition metal oxides (such as Fe_2O_3, NiO and CuO) have been investigated as anode materials for lithium-ion batteries because they show almost double the energy density of the graphite-based materials which are currently available as commercial anode materials [3–6]. Carbon composites containing the transition metal oxides have also been reported with improved cycling stability and enhanced high rate capability [7–15]. Furthermore, a new reported binder (sodium carboxymethyl cellulose, CMC) greatly enhances the cycling stability of transition metal oxide anodes [8, 14–17]. However, the commercially available electrolytes typically are flammable organic solvents, which present significant safety issues. Room temperature ionic liquids (RTILs), on the other hand are, in some cases, flame resistant, non-volatile and electrochemically stable, giving them potential as safe electrolytes in lithium-ion battery systems [18]. Recently, Ishikawa et al. [19] reported using RTILs containing bis(fluorosulfonyl)imide (FSI) as an anion, which can provide near theoretical reversible capacity for graphite-based negative electrode during repeated cycling, without any additives. Hassoun et al. [20] reported that Sn–C alloy can form a much more stable surface-protecting film than lithium metal in a RTIL based on *N*–*n*-butyl-*N*-ethyl pyrrolidinium (Py24) cations. However, there is still no report on using ionic liquid with transition metal oxide anode materials. In this article, two types of RTILs were used as electrolyte for three types of transition metal oxide/carbon composites. The RTILs used are 1-ethyl-3-methyl-imidazolium bis(fluorosulfonlyl)imide

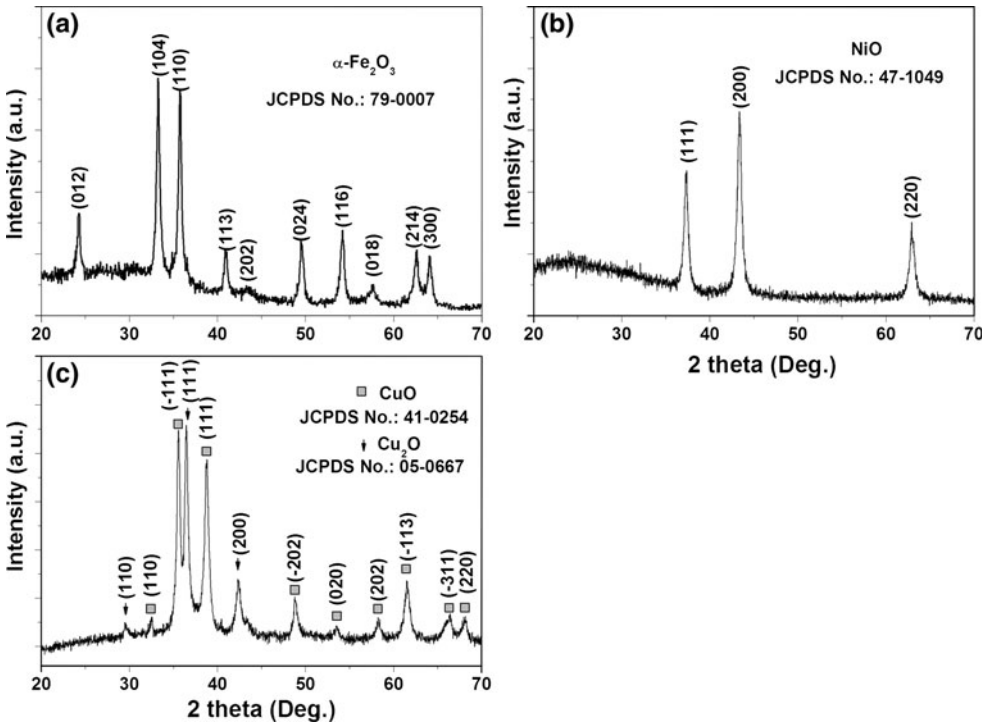

Fig. 1 XRD patterns of as-prepared Fe_2O_3/C (**a**), NiO/C (**b**) and CuO/Cu_2O/C (**c**) composites

(EMI-FSI) and 1-methyl-1-propylpyrrolidinium bis(fluorosulfonyl)imide (Py13-FSI).

2 Experimental

Fe_2O_3/C, NiO/C and CuO/Cu_2O/C composites were prepared via spray pyrolysis. The details can be found elsewhere [8, 11, 14]. The morphology and microstructure of the as-prepared Fe_2O_3/C, NiO/C and CuO/Cu_2O/C composites were characterized by X-ray diffraction (XRD; GBC MMA 017), scanning electron microscopy (SEM; JEOL JSM-7500FA) and thermogravimetric analysis (TGA; Mettler TGA/DSC). Electrochemical measurements, including charge–discharge measurements and cyclic voltammetry (CV), were obtained using a Land battery test system and an 8-channel VMP electrochemistry workstation, respectively. The electrochemical coin cells (CR 2032) that were used for testing contained the composites on Cu foil with sodium carboxymethyl cellulose (CMC) binder as the working electrode, lithium foil as the counter electrode and reference electrode, porous polypropylene as the separator and 1 M $LiN(SO_2CF_3)_2$ (LiTFSI) in RTIL as the electrolyte. The two RTILs used and compared here are 1-ethyl-3-methylimidazolium bis(fluorsulfonyl)imide (EMI-FSI) and *N*-methyl-*N* propylpyrrolidinium bis(fluorsulfonyl)imide (Py13-FSI), based on FSI anion from Dai-Ichi Kogyo, Seiyaku Co., Ltd, Japan (DKS). These RTILs contain less than 10 ppm (w/w) H_2O, and less than 2 ppm (w/w) of halide and alkali metal-ion impurities. The RTILs were used without any further treatment. The cells were galvanostatically charged and discharged in the range of 0.01–3.0 V at constant current densities of 10 mA g^{-1} for the first 5 cycles and 50 mA g^{-1} for the following cycles.

3 Results and discussion

X-ray diffraction (XRD) patterns of Fe_2O_3/C, NiO/C and CuO/Cu_2O/C composites are shown in Fig. 1. The diffraction peaks of the as-prepared Fe_2O_3/C composite in Fig. 1a can be indexed to a rhombohedral α-Fe_2O_3 phase with space group R-3c (JCPDS No. 79-0007). The peaks in the pattern of the NiO/C composite (Fig. 1b) can be attributed to cubic NiO phase with space group Fm-3 m (JCPDS No. 47-1049). In Fig. 1c, the diffraction peaks of CuO/Cu_2O/C composite can be indexed to a mixture of monoclinic structure CuO with space group C2/c (JCPDS 41-0254) and cubic structure Cu_2O with space group Pn3m (JCPDS 05-0667). The high background in all the three patterns from 20 to 40° is due to the presence of amorphous carbon. In order to approximately calculate the carbon contents, thermogravimetric analysis (TGA) was used, and the results are shown in Fig. 2. The weight loss from 200 to 350 °C can be assigned to the carbon loss. The starting temperature for the weight loss is different for each of these composites. This is probably due to the different natures of

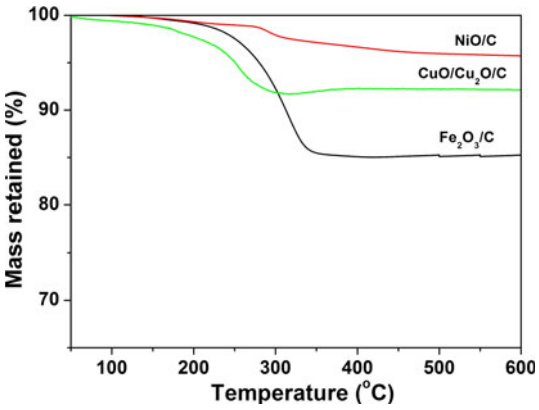

Fig. 2 TGA curves of the as-prepared Fe_2O_3/C, NiO/C and CuO/Cu_2O/C composites

the carbon and/or different catalytic properties of different transition metal oxides. The approximate carbon content for Fe_2O_3/C, NiO/C and CuO/Cu_2O/C composites is 4, 8 and 14 wt%, respectively. The TGA curve of the CuO/Cu_2O/C composite shows a weight increase of around 1% from 320 to 400 °C. This is due to the oxidation reaction from Cu_2O to CuO described in Eq. 1.

$$Cu_2O + {}^1/_2O_2 \rightarrow 2CuO \quad (1)$$

The weight increase is around 11% from Eq. 1. Therefore, we can estimate that the Cu_2O content is around 10% in the composite. The specific surface areas of the as-prepared composites were measured by the 15-point Brunauer–Emmett–Teller (BET) N_2 adsorption method. The specific surface areas of Fe_2O_3/C, NiO/C and CuO/Cu_2O/C composites are 260, 41 and 96 $m^2\ g^{-1}$, respectively. The Fe_2O_3/C composite shows a much higher surface area than the other two composites.

The SEM images of the as-prepared Fe_2O_3/C, NiO/C and CuO/Cu_2O/C composites are shown in Fig. 3. In general, all the three types of composites show hollow spherical morphology in low magnification SEM images, with the diameters of the spherical particles in the order of 1–10 μm (Fig. 3a, c, e). The diameter reflects the pore size in the nozzle. Figure 3b shows a higher magnification SEM image of the Fe_2O_3/C composite. The walls of the hollow

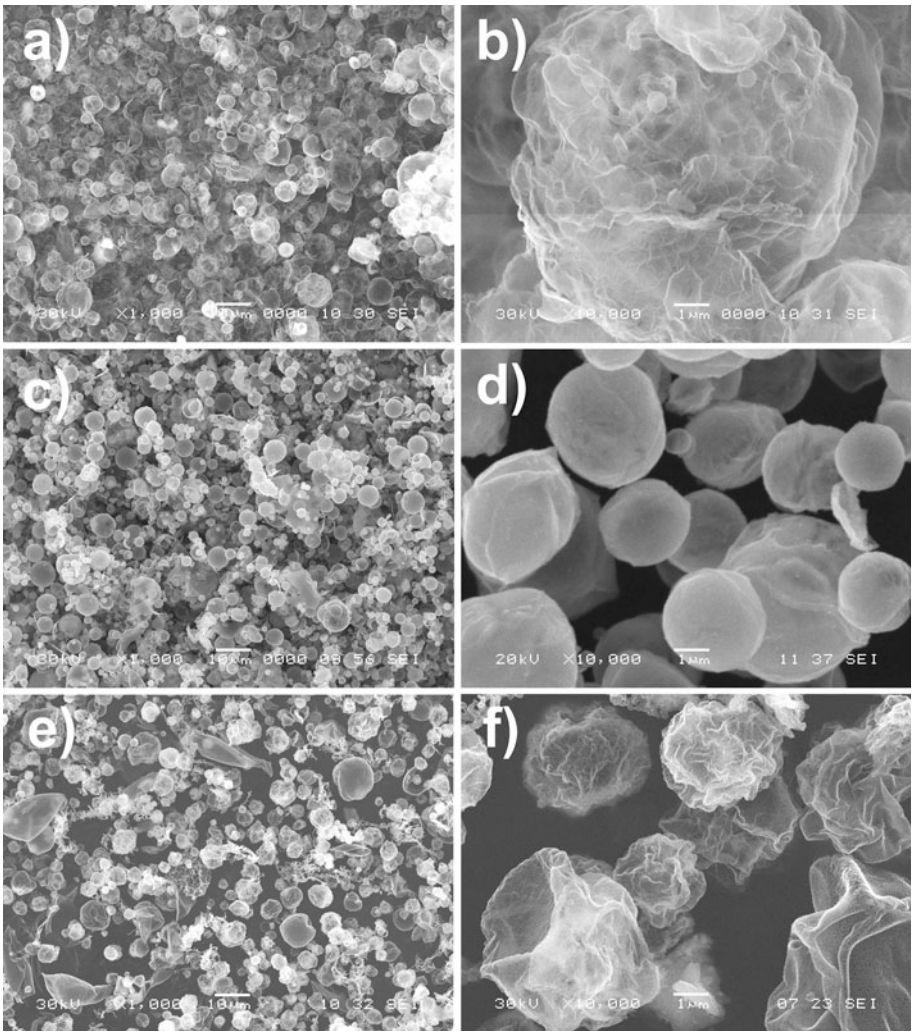

Fig. 3 SEM images of as-prepared Fe_2O_3/C (**a**, **b**), NiO/C (**c**, **d**) and CuO/Cu_2O/C (**e**, **f**) composites

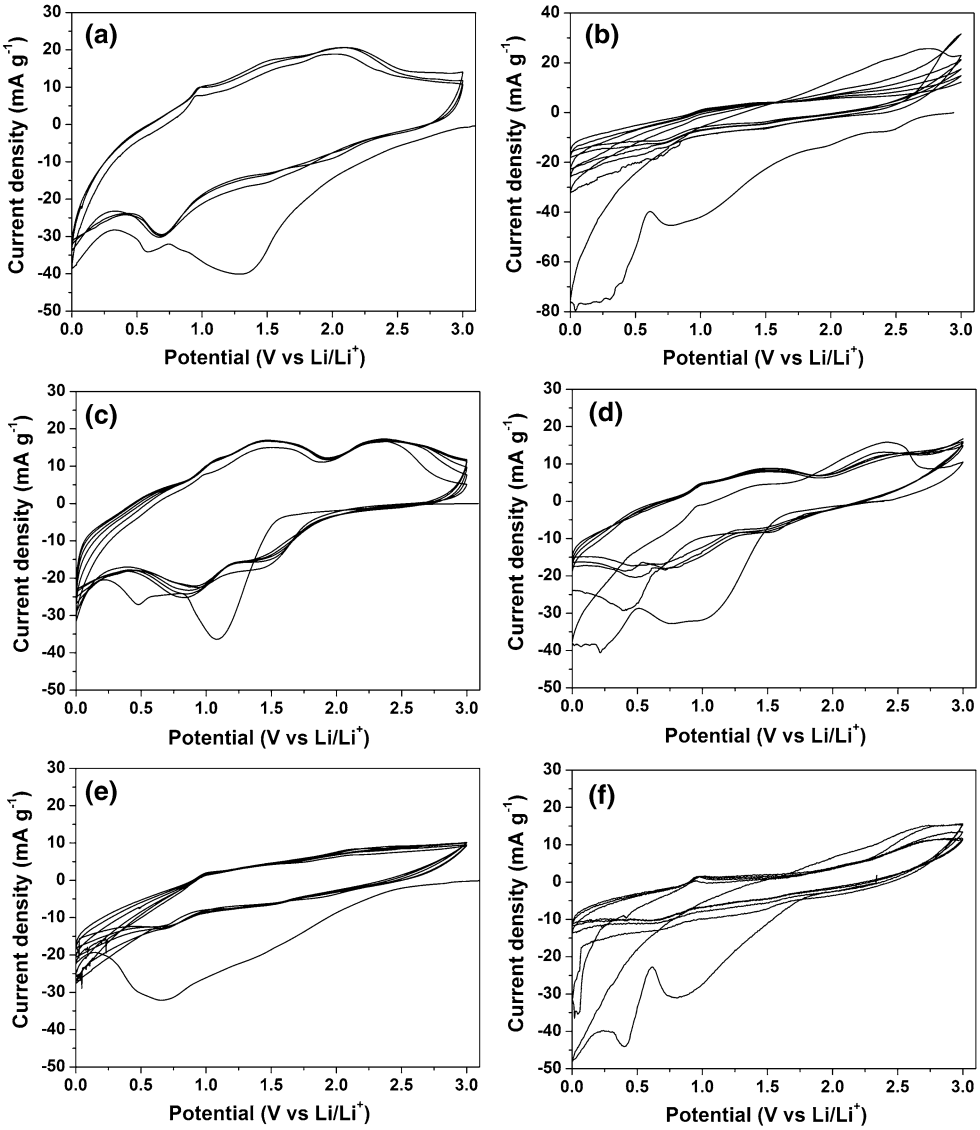

Fig. 4 Cyclic voltammograms of Fe_2O_3/C (**a**, **b**), NiO/C (**c**, **d**) and CuO/Cu_2O/C (**e**, **f**) at scan rates of 0.1 mV s^{-1} using Py13-FSI (**a**, **c**, **e**) and EMI-FSI (**b**, **d**, **f**) RTILs as electrolytes

structures are composed of very thin nanosheets around 10–20 nm in thickness, which can account for the high surface area. The NiO/C composite (Fig. 3d) shows much smoother and more condensed spherical morphology with wall thickness around 300 nm, indicating much lower surface area. Figure 3f shows a higher magnification SEM image of the CuO/Cu_2O/C composite. It can be seen that the CuO/Cu_2O/C composite has a similar morphology to the Fe_2O_3/C composite but is much more condensed than the Fe_2O_3/C composite.

The three types of transition metal oxide/carbon composites have been used as anode for lithium ion battery application using conventional electrolyte (1 M $LiPF_6$ in ethylene carbonate (EC):dimethyl carbonate (DMC) = 1:1 (v/v) or EC:diethyl carbonate (DEC) = 1:2 (v/v)), and a new binder, sodium carboxymethyl cellulose (CMC). They showed enhanced rate capability and excellent cycling stability [8, 11, 14]. Here, two types of RTILs were used as electrolyte for all the three types of transition metal oxide/carbon composites; these were 1-ethyl-3-methyl-imidazolium bis(fluorosulfonlyl)imide (EMI-FSI) and 1-methyl-1-propylpyrrolidinium bis(fluorosulfonyl)imide (Py13-FSI). Figure 4 displays cyclic voltammograms of composite materials using the two RTILs as electrolyte at a scan rate of 0.1 mV s^{-1} between 0.0 and 3.0 V. The reactions between the lithium and transition metal oxide have been proposed before [3] and are listed as Eqs. 2–4.

Initial discharge (lithiation):

$$M_xO_y + 2y\ Li^+ + 2y\ e^- \rightarrow xM + yLi_2O \quad (2)$$

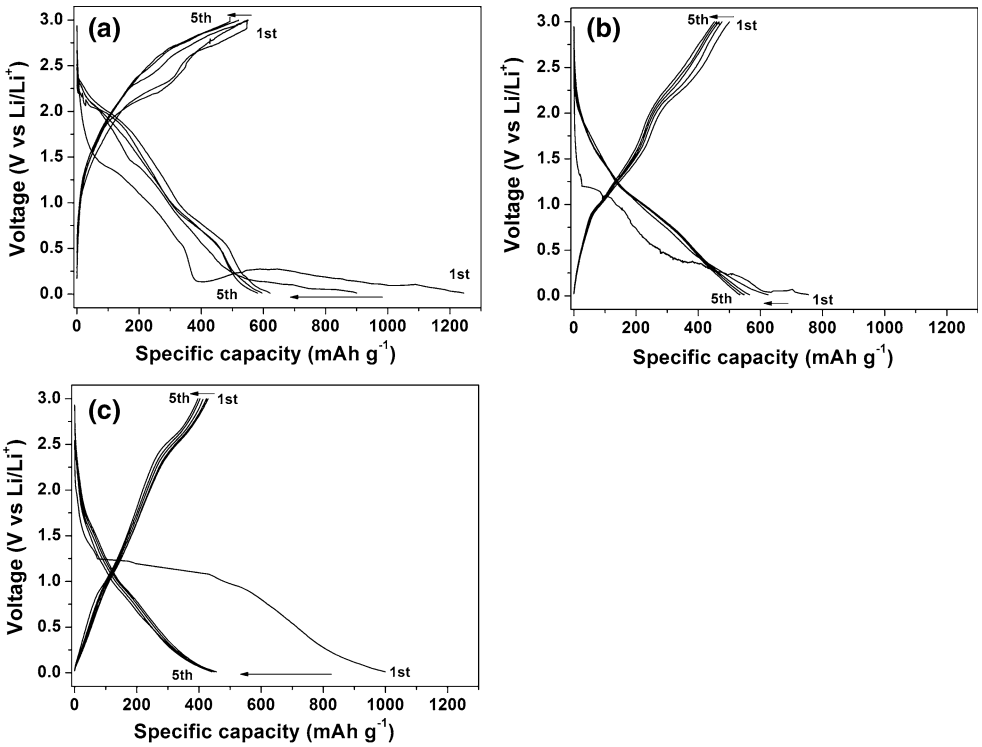

Fig. 5 Typical charge–discharge curves of Fe_2O_3/C (**a**), NiO/C (**b**) and CuO/Cu_2O/C (**c**) composites using Py13-FSI ionic liquid as electrolyte

Charge (delithiation):

$$xM + zLi_2O \rightarrow M_xO_z + 2zLi^+ + 2ze^- \quad (3)$$

Discharge (lithiation):

$$M_xO_z + 2zLi^+ + 2ze^- \rightarrow xM + zLi_2O \quad (x,\ y,\ z = 1,\ 2,\ \ldots n) \quad (4)$$

In the first cycle, the maximum cathodic current peak between 0.5 and 1.1 V is due to the formation of the solid electrolyte interphase (SEI) layer and the reduction of the metal oxide. The different steps indicate the multistep reactions due to the multiple changes in chemical valence. The intensities of the cathodic peaks decreased in the subsequent scanning cycles due to the irreversible reaction 2 and the formation of the SEI film. The composite electrodes using Py13-FSI as electrolyte show much better electrochemical performance than those using EMI-FSI as electrolyte, in terms of the peak intensity and reversibility. Previous reports [19, 21] show that EMI-FSI can be successfully used as electrolyte for both graphite and Si/Ni/C composite materials with relatively good performance. However, poor electrochemical performance of transition metal oxides was observed when using EMI-FSI as electrolyte, as shown in Fig. 4b, d and f. This is probably due to the catalytic effects of the transition metal oxides, which make the EMI-FSI or the as-formed SEI layer unstable. In Fig. 4a, c and e, the intensities of the cathodic peaks in the following cycles are in the order of $I_{Fe2O3/C} > I_{NiO/C} > I_{CuO/Cu2O/C}$, indicating that the discharge capacities should be in the same order. From the second cycle to the fifth cycle, the intensity of the cathodic peak (at around 0.6 V) of the Fe_2O_3/C composite remains the same, so that this composite shows the best cycling stability among all the samples. The anodic peaks are very broad and were not very clearly observed for the CuO/Cu_2O/C composite. Three small anodic peaks could be seen in the potential range from 1.0 to 2.5 V for both the Fe_2O_3/C and the NiO/C composites. The cathodic and anodic peaks with Py13-FSI used as electrolyte are all shifted to lower and higher potentials, respectively, compared with those observed in conventional electrolyte. This is probably due to the much higher viscosity of the RTILs, combined with worse wettability, compared with conventional electrolyte at room temperature [22], and also the strong catalytic effect of the transition metal oxides.

Typical discharge–charge curves of the Fe_2O_3/C, NiO/C and CuO/Cu_2O/C composite electrodes in coin cells are shown in Fig. 5. The composite materials using RTILs show very different initial discharge curves from those using conventional electrolyte in previous reports [8, 11, 14]. The initial discharge capacities for Fe_2O_3/C, NiO/C and CuO/Cu_2O/C composites are 1250, 750 and 1000 mAh g^{-1}, respectively. The second discharge capacities for Fe_2O_3/C, NiO/C and CuO/Cu_2O/C composites are 620, 570 and 450 mAh g^{-1}, respectively. The main reasons for the existence of the initial irreversible capacity in anode materials

are the formation of a SEI layer and the irreversible reaction during the first discharge. Fe_2O_3/C composite using Py13-FSI as electrolyte shows the highest discharge capacity, in good agreement with the CV tests.

Figure 6 displays the effect of cycling on the Fe_2O_3/C, NiO/C and CuO/Cu_2O/C composite electrodes at a current density of 10 mA g^{-1} for the first 5 cycles and 50 mA g^{-1} for the following cycles. After 5 cycles, Fe_2O_3/C, NiO/C and CuO/Cu_2O/C composite electrodes show an almost stable capacity of 581, 533 and 448 mAh g^{-1}, respectively. When the current density changes to 50 mA g^{-1}, the Fe_2O_3/C, NiO/C and CuO/Cu_2O/C composite electrodes show specific capacities of ~420, ~370 and ~210 mAh g^{-1}, respectively. The capacity can be maintained up to 50 cycles for the Fe_2O_3/C and CuO/Cu_2O/C composites. The NiO/C composite electrode shows a gradual drop in capacity to 200 mAh g^{-1} after 50 cycles. It is worth pointing out that Fe_2O_3/C composite shows the highest specific capacity (425 mAh g^{-1}) and the best capacity retention up to 50 cycles under the higher current density (50 mA g^{-1}). This may be due to the higher theoretical capacity of Fe_2O_3 compared with NiO and CuO/Cu_2O, and the much higher surface area of Fe_2O_3/C, which increases the contact surface between the RTIL and the active materials. Therefore, the electrochemical performance is much better than those of the NiO/C and CuO/Cu_2O/C composites. The cycle life of nano-Fe_2O_3 and commercial Fe_2O_3 electrode are also presented here for comparison. The nano-Fe_2O_3 was also prepared by spray pyrolysis at 1,000 °C. The experimental details and characterization can be found in a previous report [8]. The commercial α-Fe_2O_3 was purchased from Sigma-Aldrich and has a surface area of less than 10 m^2 g^{-1}. From the results, the commercial α-Fe_2O_3 only shows a small initial discharge capacity of 244 mAh g^{-1} and a stable discharge capacity around 80 mAh g^{-1} at a current density of 50 mA g^{-1}. This indicates that the surface area is an important factor affecting the performance of Fe_2O_3. It can also be seen in Fig. 6 that nano-Fe_2O_3 has a similar discharge capacity to that of Fe_2O_3/C composite at a current density of 10 mA g^{-1} but it only shows a capacity below 300 mAh g^{-1} when the current was changed to 50 mA g^{-1}, indicating that the carbon composite is also important for good capacity retention and good high rate capability. These results are in good agreement with our previous report in which conventional electrolyte was used. In addition, because of the poorer wettability and lower ionic conductivity of RTILs at room temperature, the capacities of composites in RTILs are much lower than in the conventional electrolytes [8, 11, 14].

Figure 7 shows the Nyquist plots of the nano-Fe_2O_3 and Fe_2O_3/C composite electrodes at a discharge potential of 0.85 V versus Li/Li^+ after charge and discharge for 5 cycles. The impedance curves show one compressed semicircle in the medium-frequency region, which could be assigned to charge transfer resistance (R_{ct}), and an approximately 45° inclined line in the low-frequency range, which is related to the Warburg impedance. The R_{ct} of nano-Fe_2O_3 and Fe_2O_3/C composite is 1,250 and 880 Ω, respectively. The intercepts on the real axis Z' could be considered as representing the combined resistance, including the ionic resistance of the electrolyte, the intrinsic resistance of the active materials and the contact resistance at the active material/current collector interface. The combined resistance for nano-Fe_2O_3 and Fe_2O_3/C is 420 and 328 Ω, respectively. The carbon composite shows both lower R_{ct} and lower combined resistance. However, all these values are at least one order of magnitude higher than those in the conventional electrolyte [23]. This is still a big disadvantage of using ionic liquid as electrolyte in the lithium-ion battery at room temperature. The study

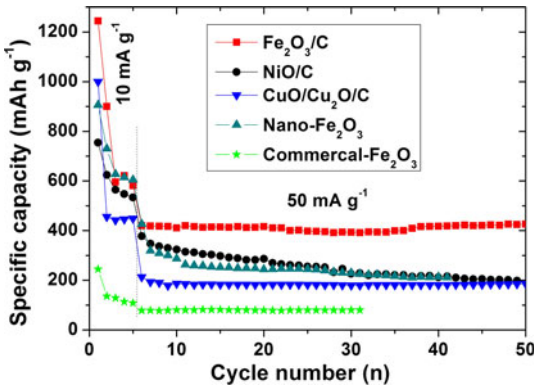

Fig. 6 Cycle life of Fe_2O_3/C, NiO/C, CuO/Cu_2O/C, nano-Fe_2O_3 and commercial Fe_2O_3 electrodes using Py13-FSI ionic liquid as electrolyte at a current density of 10 mA g^{-1} for the first 5 cycles and 50 mA g^{-1} for the rest of the cycles

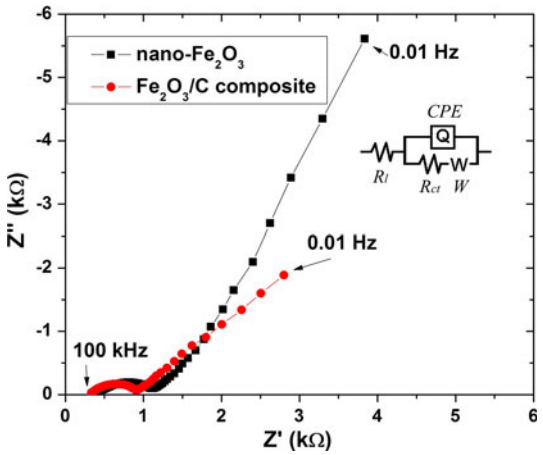

Fig. 7 Nyquist plots of nano-Fe_2O_3 and Fe_2O_3/C composite electrodes at a discharge potential of 0.85 V (vs. Li/Li^+) from 100 kHz to 10 mHz

presented here is just the preliminary results. Further study that is still ongoing in our group includes optimizing the surface area and carbon content, and selecting different ionic liquids to improve the ionic conductivity.

4 Conclusions

Three types of transition metal oxide/carbon composites, synthesized by spray pyrolysis, have been used as anode for lithium ion battery application in two types of ionic liquid electrolyte: 1 M LiTFSI in 1-ethyl-3-methyl-imidazolium bis(fluorosulfonlyl)imide (EMI-FSI) or 1-methyl-1-propylpyrrolidinium bis(fluorosulfonyl)imide (Py13-FSI). The electrochemical measurements show that the composite electrodes using Py13-FSI as electrolyte have much better electrochemical performance than those using EMI-FSI in terms of capacity and reversibility. The Fe_2O_3/C composite shows the highest specific capacity and the best capacity retention under higher current density (50 mA g^{-1}) up to 50 cycles, compared with the NiO/C and CuO/Cu_2O/C composites. These preliminary results show that Py13-FSI could be used as an electrolyte for transition metal oxides in lithium-ion batteries. More study is needed to understand the catalytic effects of transition metal oxides in the RTILs and to further improve the electrochemical performance.

Acknowledgments Financial support provided by the Australian Research Council (ARC) through a Discovery Project (DP 0987805) and ARC Centre of Excellence funding (CE0561616) is gratefully acknowledged. The authors thank Dr. T. Silver at the University of Wollongong for critical reading of the manuscript.

References

1. Yoshio M, Brodd RJ, Kozawa A (2009) Lithium-ion batteries: science and technologies. Springer Press, New York Chapter 1
2. Tarascon JM, Armand M (2001) Nature 414:359
3. Poizot P, Laruelle S, Grugeon S, Dupont L, Tarascon JM (2000) Nature 407:496
4. Chen J, Xu LN, Li WY, Gou XL (2005) Adv Mater 17:582
5. Varghese B, Reddy MV, Yanwu Z, Lit CS, Hoong TC, Rao GVS, Chowdari BVR, Wee ATS, Lim CT, Sow CH (2008) Chem Mater 20:3360
6. Grugeon S, Laruelle S, Herrera-Urbina R, Dupont L, Poizot P, Tarascon JM (2001) J Electrochem Soc 148:A285
7. Jiao F, Bao J, Bruce PG (2007) Electrochem Solid-State Lett 10:A264
8. Chou SL, Wang JZ, Wexler D, Konstantinov K, Zhong C, Liu HK, Dou SX (2010) J Mater Chem 20:2092
9. Huang XH, Tu JP, Zhang CQ, Chen XT, Yuan YF, Wu HM (2007) Electrochim Acta 52:4177
10. Fu LJ, Liu H, Zhang HP, Li C, Zhang T, Wu YP, Holze R, Wu HQ (2006) Electrochem Commun 8:1
11. Rahman MM, Chou SL, Zhong C, Wang JZ, Wexler D, Liu HK (2010) Solid State Ion 180:1646
12. Wu GT, Wang CS, Zhang XB, Yang HS, Qi ZF, Li WZ (1998) J Power Sources 75:175
13. Xiang JY, Tu JP, Zhang J, Zhong J, Zhang D, Cheng JP (2010) Electrochem Commun 12:1103
14. Zhong C, Wang JZ, Gao XW, Chou SL, Konstantinov K, Liu HK (2011), J Nanosci Nanotechnol Accepted
15. Wang JZ, Zhong C, Wexler D, Idris NH, Wang ZX, Chen LQ, Liu HK (2011) Chem Eur J 17:661
16. Li J, Dahn HM, Krause LJ, Le DB, Dahn JR (2008) J Electrochem Soc 155:A812
17. Zhong C, Wang JZ, Chou SL, Konstantinov K, Rahman M, Liu HK (2010) J Appl Electrochem 40:1415
18. Galinski M, Lewandowski A, Stepniak I (2006) Electrochim Acta 51:5567
19. Ishikawa M, Sugimoto T, Kikuta M, Ishiko E, Kono M (2006) J Power Sources 162:658
20. Hassoun J, Fernicola A, Navarra MA, Panero S, Scrosati B (2010) J Power Sources 195:574
21. Sugimoto T, Atsumi Y, Kono M, Kikuta M, Ishiko E, Yamagata M, Ishikawa M (2010) J Power Sources 195:6153
22. Guerfi A, Duchesne S, Kobayashi Y, Vijh A, Zaghib K (2008) J Power Sources 175:866
23. Chou SL, Wang JZ, Chen ZX, Liu HK, Dou SX (2011) Nanotechnology 22:265401